

## PRELIMINARY TESTS AT THE UNIVERSITY OF OTTAWA SUPERCRITICAL CO<sub>2</sub> HEAT TRANSFER FACILITY

L. Jeddi, K. Jiang, S. Tavoularis and D.C. Groeneveld  
University of Ottawa, Ontario, Canada

### Abstract

This article describes the new supercritical heat transfer test facility that has been constructed at the University of Ottawa and preliminary tests for its commissioning. The facility uses CO<sub>2</sub> as a medium and has three test sections: a tube with an 8 mm ID, to serve as a reference for comparisons with literature, a second tube with a 22 mm ID, and a rod bundle. The facility is designed for tests in the ranges of pressure, heat flux and mass flux that correspond to normal, enhanced and deteriorated heat transfer under conditions relevant to supercritical water cooled reactor designs. Some preliminary measurements of the heat transfer coefficient under subcritical and supercritical conditions in the 8 mm tube are presented and compared to representative correlations. This article also discusses plans for heat transfer measurements in the rod bundle and measurements of turbulence properties and temperature fluctuations using hot- and cold-wire probes in the 22 mm tube.

### 1. Introduction

The present research is in support of the Canadian National Program on Generation IV Energy Technologies for the development of a Super Critical Water-cooled Reactor (SCWR), which, compared to existing nuclear reactors, is expected to have increased safety, lower-cost electricity production, more compact size and reduced volume of nuclear wastes. The operation of such reactors requires heat transfer to the cooling fluid at pressures higher than the critical pressure. At this pressure, the heat transfer behaviour is quite different from that at subcritical pressure because of the drastic variations of the physical properties near the pseudo-critical temperature [1]. Thus, an accurate prediction of the heat transfer coefficient is necessary for a thermal-hydraulic reactor design.

A heat transfer test facility which can be operated at subcritical and supercritical pressures using carbon dioxide as a surrogate for water has been built at the University of Ottawa. Carbon dioxide was chosen as working fluid because of its inertness and its lower critical pressure and temperature compared to those of water (see Table 1); this reduced the safety requirements as well as the loop construction and operating costs. The following sections describe the loop and provide some preliminary results for heat transfer in an 8 mm tube at two different pressures. The heat transfer coefficients estimated from the tests are compared with corresponding predictions of existing heat transfer correlations.

Table 1 Critical conditions for water and carbon dioxide.

Parameter	Symbol	Unit	H <sub>2</sub> O	CO <sub>2</sub>
Critical pressure	$P_c$	MPa	22.1	7.4
Critical temperature	$T_c$	°C	374.1	31.0
Critical density	$\rho_c$	kg m <sup>-3</sup>	315	468

## 2. Test facility

### 2.1 General description of the loop

A schematic diagram of the loop is shown in Figure 1. The loop was designed for a maximum pressure of 15 MPa and a nominal operating pressure of 10 MPa.

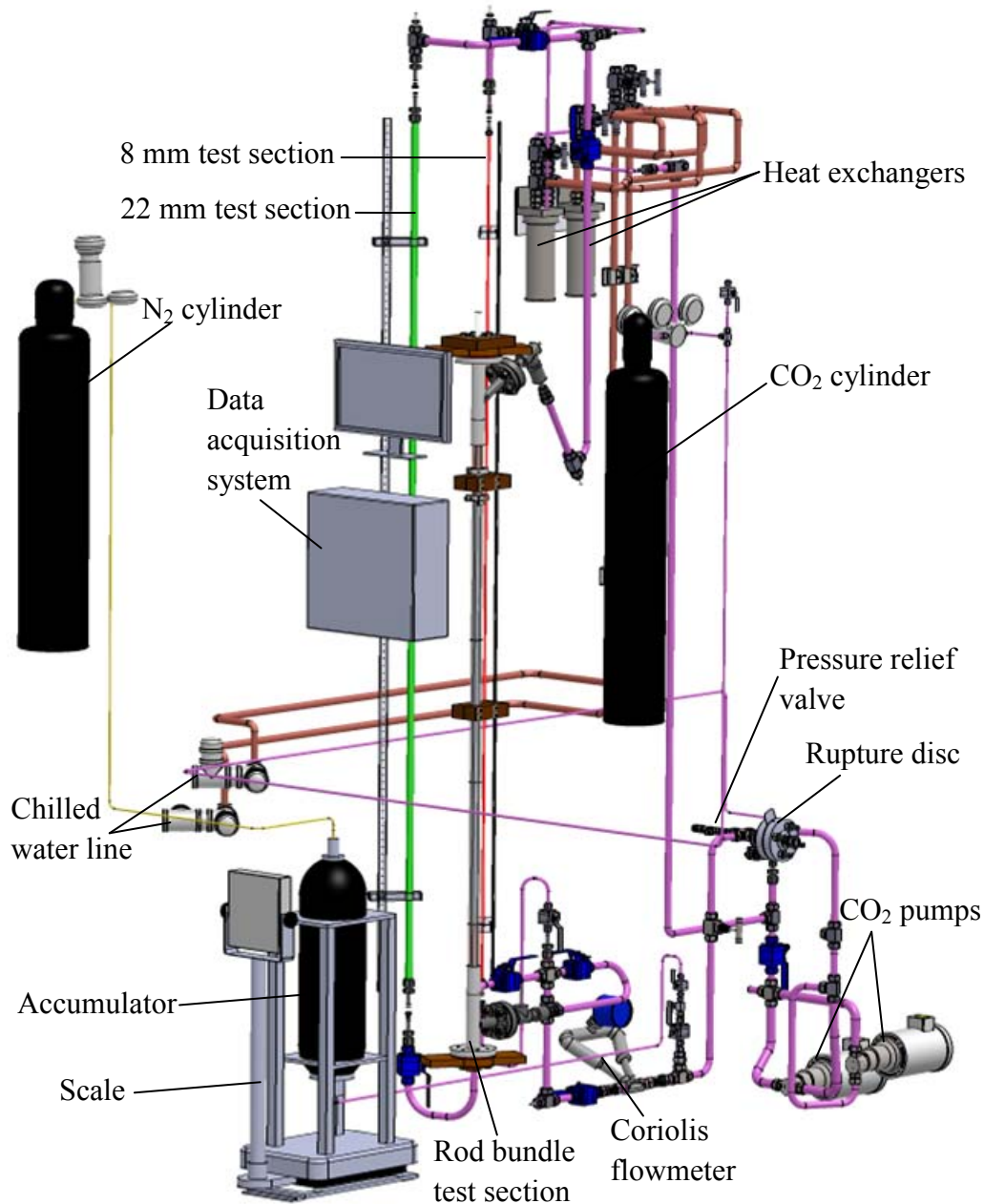


Figure 1 Schematic diagram of the supercritical CO<sub>2</sub> loop.

The loop is filled with CO<sub>2</sub> from cylinders with an internal pressure of 13 MPa through a regulating valve. CO<sub>2</sub> flow is driven by a gear pump (Cole-Palmer, Model GLH23.JVS;E.M2N1CH15). A second

pump is available for operation in parallel with the first one so that higher flow rates can be achieved; additional pumps can be installed for even higher flow rates. A gear pump design was adopted to keep flow fluctuations as low as possible.

A bladder accumulator is used to maintain the loop pressure at the desired value during its operation. The inner side of the bladder is connected to a pressurized nitrogen cylinder, whereas its outer side is connected to the CO<sub>2</sub> in the loop downstream of the pump. The accumulator is mounted on a scale so that the weight of liquid or liquid-like CO<sub>2</sub> in it can be monitored.

The flow rate in the loop is regulated by adjusting the pump speed using a single inverter (Cole-Parmer, Model 3PH Nema 4VFD7.5HP). A pressure relief device and a rupture disc are installed to prevent over-pressurization of the loop.

The test sections are heated electrically by passing direct current through their walls; power is provided by a DC power supply rated at a maximum voltage of 60 V and a maximum current of 2833 A.

The CO<sub>2</sub> leaving the test section is cooled by passing through two single helical tube heat exchangers (Sentry Equipment Corp., Model FXF-6223U) connected in series. In this preliminary stage of the tests, the secondary sides of both heat exchangers are connected to the central chilled water supply, whose specifications are summarized in Table 2. In later stages of the work, and in order to reach lower test section inlet temperatures, the second heat exchanger will use Dowtherm J synthetic organic heat transfer fluid (Dow Chemical Co.), which has a relatively low viscosity at low temperatures (e.g.,  $1.8 \times 10^{-3} \text{ kg m}^{-1} \text{ s}^{-1}$  at -20 °C; this value is much lower than that of glycol or other commonly used low-temperature liquids); nominal specifications for this coolant are also presented in Table 2. The Dowtherm J fluid is stored in a tank in a walk-in freezer (Figure 2) and pumped to the CO<sub>2</sub> loop using a low-temperature pump (Dynapump Corp., Model JSB-2HP-1S, rated at 75 l/min). The same fluid is recirculated by a separate pump (Dynapump Corp., Model JSB-2HP-1S, rated at 38 l/min) to two radiators (Heat Innovations, Inc., 2-Row, 36x36) inside the freezer to maintain its temperature at a low level. Both pumps are located outside the walk-in freezer. All coolant supply lines are thermally insulated to keep heat losses to the surroundings as low as possible.

Table 2 Cooling system specifications.

Parameter	Unit	Nominal Value
Chilled water system:		
Inlet temperature	°C	10 (winter), 5 (summer)
Flow rate	l/min	166
Cooling capacity	kW	215 (winter), 274 (summer)
Dowtherm J system:		
Inlet temperature	°C	-35 (higher for continuous operation)
Flow rate	l/min	180
Cooling capacity	kW	92

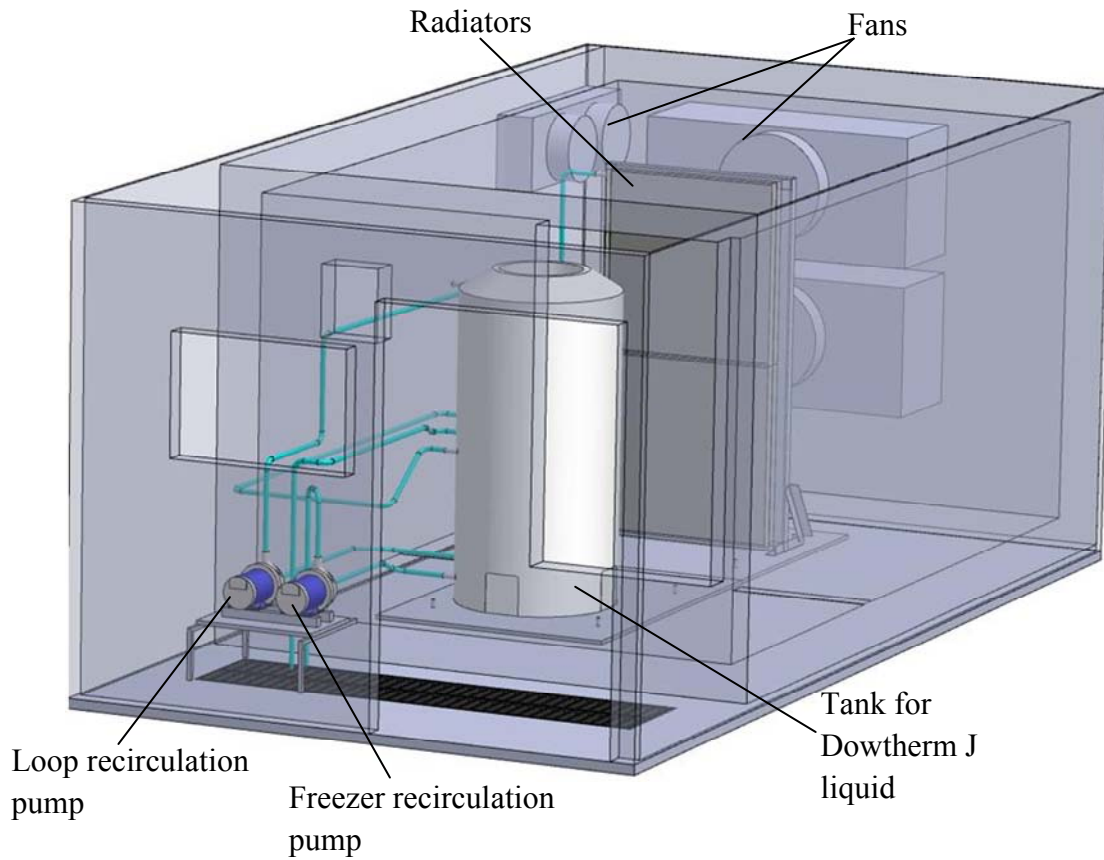


Figure 2 Schematic diagram of the walk-in freezer and the secondary cooling system.

## 2.2 Test section design

Three interchangeable test sections are connected to the loop: a tube with an 8 mm ID, a second tube with a 22 mm ID, and a rod bundle, all mounted vertically for upward flow. Figure 3 shows the first test section design, which consists of a circular tube made of Inconel 625 with an ID of  $D = 8.0$  mm, a wall thickness of 1.0 mm and a length of 3.05 m. This tube is connected to the loop using electrically insulating connectors and to the power supply using two clamped electric terminals, whose position along the tube can be adjusted. The nominal heated length of the tube was  $L_h = 1.87$  m and follows an unheated length of at least 1 m (i.e., 125 diameters), which allows the flow to develop without complications due to heating.

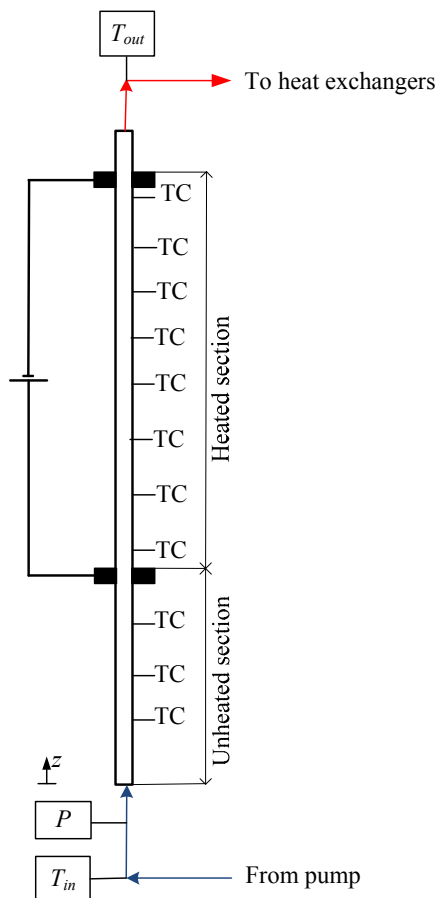


Figure 3 Schematic diagram of the 8 mm tube test section.

### 2.3 Instrumentation

For the particular tests reported here, 11 T-type thermocouples (Omega Engineering, Inc., Model SA1XL-T-SRTC) were installed along the 8 mm tube test section at distances of 254 mm from each other. For the main tests, many more thermocouples, as well as several RTDs, will be installed along each of the two tubes. The CO<sub>2</sub> temperatures  $T_{in}$  at the inlet and  $T_{out}$  at the outlet of each of the three test sections are measured by platinum, ultra-precise, long-stem RTDs (Omega Engineering, Inc., Model P-M-1/10-8-5-1/2-G-15). The pressure in the loop is measured using a pressure transducer (Omega Engineering, Inc., Model PX01C1-3KA5T), which is installed near the inlets of the three test sections. A Coriolis-type flow meter (Micro Motion, Model CFM050M320N0A2E2ZZ) is also installed near the inlets of the test sections to measure the mass flow rate. The ranges and uncertainties of these instruments are summarized in Table 4.

Table 4 Instrument range and uncertainty.

Instrument	Unit	Range	Uncertainty
Coriolis flow meter	kg s <sup>-1</sup>	0 – 25	0.05%
Thermocouples	°C	-73 – 260	0.5 (to be reduced by calibration)
In-flow RTDs	°C	-73 – 400	0.03 + 0.0005 T
Pressure transducer	MPa	0 – 20	0.05%

## 2.4 Data collection

All signals from the sensors, the flowmeter and the scale are monitored, recorded and processed using a dedicated data acquisition and processing system (National Instruments) along with a Labview 2009 software interface. This system consists of a 1.73 GHz quad-core embedded controller ((NI PXIE-8133) installed in a PXIE 1065 chassis that can hold up to 18 modules. Currently, there are three 32 channel thermocouple modules (NI PXI 4353) used for temperature measurement, three high precision temperature and voltage modules (NI PXI 4351) used for temperature measurement with RTDs and one high-accuracy multifunction M Series data acquisition (DAQ) module (NI PXI 6289) used for voltage measurement (flowmeter, pressure transducer and scale).

## 3. Preliminary loop commissioning tests

In the following, we will present three sets of preliminary measurements collected during pilot tests in preparation for the loop commissioning. Shortly after these measurements were taken, equipment malfunction interrupted the testing. The reaction of supercritical CO<sub>2</sub> with some materials in the pumps and the accumulator and the presence of undesirable gas in the loop have been investigated among the possible sources of problems and are currently being eliminated so that loop operation may resume in the near future.

### 3.1 Test conditions

The test conditions are summarized in Table 5. These include the loop pressure  $P$  and its ratio with the critical pressure  $P_c$ , the inlet temperature  $T_{in}$ , the mass flux  $G$  and the heat flux  $q$ . Tests A and B were at a subcritical pressure and test C was at a supercritical one. The saturation temperature  $T_{sat}$  for the subcritical tests and the pseudo-critical temperature  $T_{pc}$  for the supercritical tests have also been included in Table 5. In all cases, the mass flux was kept at the same moderate value, whereas the heat flux was adjusted so that different heat transfer regimes could be examined.

Table 5 Conditions for the present tests.

Parameter	Units	Test A	Test B	Test C
$P$	MPa	6.70	6.70	7.68
$P/P_c$	-	0.90	0.90	1.04
$T_{in}$	°C	7.84	8.15	8.74
$T_{sat}$	°C	26.76	26.76	–
$T_{pc}$	°C	–	–	32.75
$G$	kg/m <sup>2</sup> s	500	500	500
$q$	kW/m <sup>2</sup>	5	50	90

### 3.2 Data reduction

The local thermophysical properties of CO<sub>2</sub> at the loop pressure and the local bulk fluid temperature were calculated using NIST software RefProp 7.0. The bulk temperature  $T_b$  of CO<sub>2</sub> at each downstream location in the tube was calculated from the loop pressure and the local bulk specific enthalpy  $i_b$  of the fluid. The bulk specific enthalpy for all three tests was assumed to increase linearly along the flow direction, as

$$i_b = \frac{(i_{out} - i_{in})}{L_h} z + i_{in} \quad (1)$$

Analysis taking into account heat conduction through the tube wall demonstrated that the temperature difference between the inner and outer wall surfaces was much lower than the overall temperature measurement uncertainty. The heat transfer coefficient  $h$  was estimated as

$$h = \frac{q \pm q_{loss}}{T_w - T_b} \quad (2)$$

for the cases for which no boiling was detected to occur and as

$$h = \frac{q \pm q_{loss}}{T_w - T_{sat}} \quad (3)$$

for cases for which boiling was present. Because during these specific preliminary tests the test section was not insulated, there was heat transfer to or from the surroundings and so a rough estimate of heat flux  $q_{loss}$  to or from the exterior of the tube was used to correct the estimate of  $h$ .

### 3.3 Heat transfer correlations used for comparisons

At this preliminary stage of the work, we present comparisons of our results with representative correlations for subcritical and supercritical pressures. For forced convection in circular tubes at subcritical pressures, we considered the widely used Dittus-Boelter (D-B) correlation [2]:

$$Nu_b = 0.0243 Re_b^{0.8} Pr_b^{0.4} \quad (4)$$

When it was assessed that film boiling occurred in the tube, the following Dougall-Rohsenow (D-R) form of the D-B correlation was used

$$Nu_{fb} = hD / k_v = 0.0243 Re_{hom}^{0.8} Pr_v^{0.4} \quad (5)$$

where the Reynolds number for homogeneous fluid is

$$Re_{hom} = \frac{GD}{\mu_g} \left[ x_e + (1 - x_e) \frac{\rho_g}{\rho_f} \right] \quad (6)$$

For supercritical pressures, we considered as representative the correlation devised by Jackson and Fewster (J-F correlation) [3]:

$$Nu_b = 0.0183 Re_b^{0.82} \overline{Pr}_b^{0.5} \left( \frac{\rho_w}{\rho_b} \right)^{0.3} \quad (7)$$

All symbols used in these correlations are defined in the nomenclature.

#### 4. Preliminary results

Figures 4, 5 and 6 present measurements of the wall temperatures and estimates of the heat transfer coefficients in the 8 mm tube test section for tests A, B and C, respectively, under conditions summarized in Table 5. Corresponding predictions of correlations for the heat transfer coefficients are also presented in these figures.

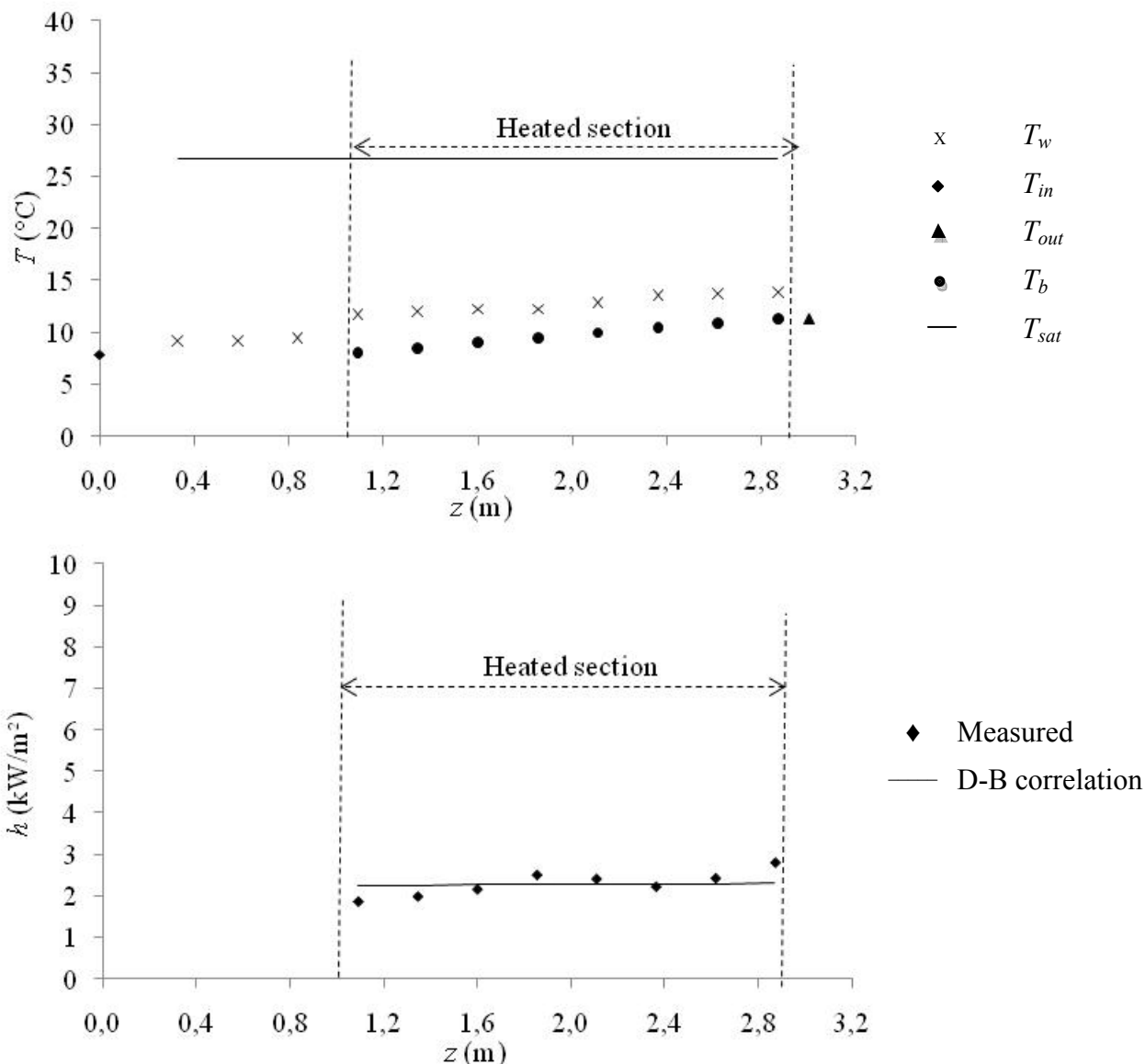


Figure 4 Measured wall temperatures and estimated heat transfer coefficients for subcritical test A (see Table 5 for test conditions).

During subcritical test A, the heat flux was sufficiently low for the wall temperature and the bulk temperature of CO<sub>2</sub> to be significantly lower than the saturation temperature (Figure 4). Consequently, the CO<sub>2</sub> remained a subcooled liquid at the exit of the test section and the heat transfer was within the normal regime for single-phase flow. The heat transfer coefficients estimated from the experimental data were in fair agreement with predictions of the Dittus-Boelter correlation.

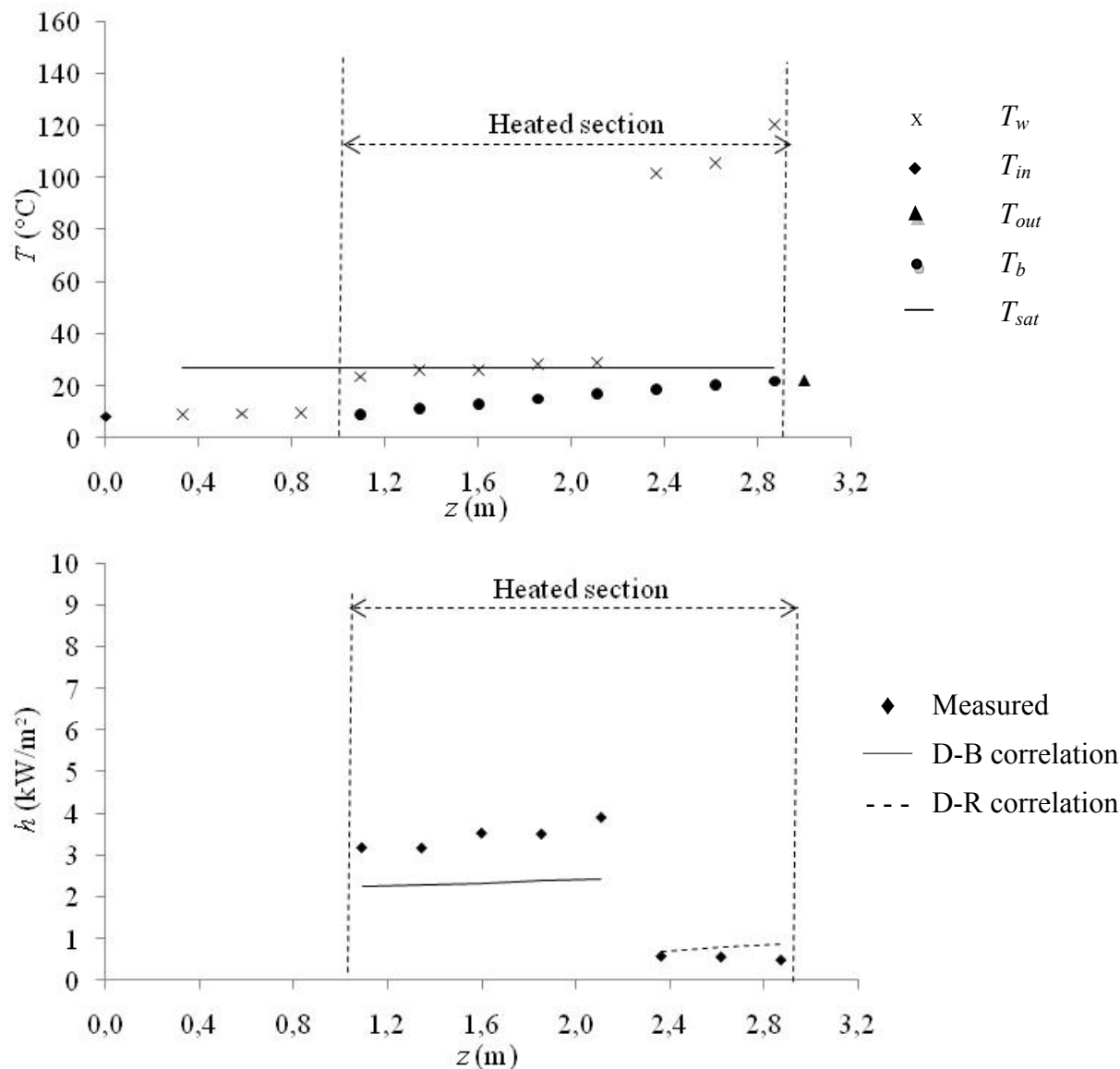


Figure 5 Measured wall temperatures and estimated heat transfer coefficients for subcritical test B (see Table 5 for test conditions).

During subcritical test B, which is at a much higher heat flux than test A, it is evident that, at a certain elevation, the heated wall temperature that exceeded the saturation temperature (Figure 5). For axial locations  $0.8 < z < 2.2$  m, the heat transfer coefficient was significantly higher than the Dittus-Boelter prediction, which indicates the presence of pre-CHF boiling. The measurements suggest that CHF occurred at  $z = 2.2$  m, because the wall temperature profile displayed a temperature rise that is typical of initiation of film boiling heat transfer. At locations  $2.2 < z < 2.9$  m, developing film boiling conditions prevailed. The experimental film boiling heat transfer coefficient and the one calculated from the D-R correlation are in fair agreement.

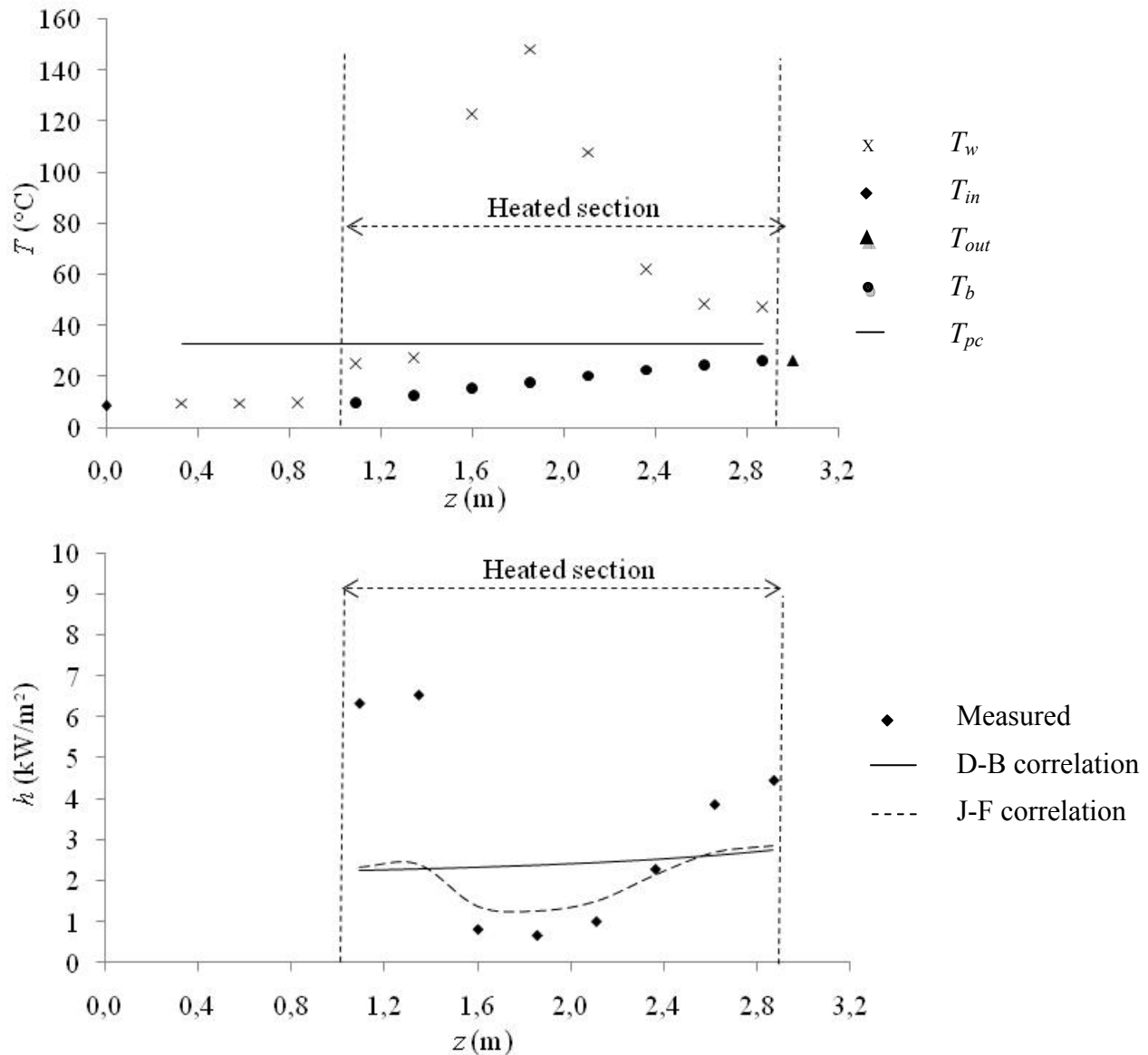


Figure 6 Measured wall temperatures and estimated heat transfer coefficients for supercritical test C (see Table 5 for test conditions).

Figure 6 shows the wall temperatures and the heat transfer coefficients for the supercritical test C. It is shown that these coefficients were relatively high near the inlet of the heated section, where the wall temperature and the bulk temperature of  $\text{CO}_2$  were both lower than the pseudo-critical temperature. Further downstream, the heat transfer deteriorated and the wall temperature exceeded the pseudo-critical temperature while the bulk temperature remained below the pseudo-critical value. The Dittus-Boelter correlation deviated from the experimental results both in values and trend, whereas the predictions of the Jackson and Fewster correlation have some qualitative resemblance with the measurements, but also deviated in values.

## 5. Ongoing work

### 5.1 Loop commissioning tests

The installation of additional instrumentation and controls is in progress. To refine the measurement resolution, additional T-type thermocouples and also wall RTDs (RDF Corp., Model 29223 - three-wire type) are being installed along the 8 mm tube at distances of 50 mm from each other. To reduce the measurement uncertainty, the thermocouples will be calibrated against the wall RTDs. In addition, a differential pressure transmitter (Omega Engineering, Inc., Model PX771A-300WCDI) will be installed to measure the pressure drop from the inlet to the outlet of the test section.

As part of the loop commissioning process, a series of tests using the 8 mm tube will be performed for a few additional representative sets of conditions, within the nominal ranges which have been summarized in Table 6. Heat balance tests will be conducted for each test by comparing electrical power input into the test section with thermal power given to the fluid, determined from the flow rate, loop pressure and enthalpy rise across the test section.

Table 6 Proposed test conditions.

Parameter	Unit	Range for CO <sub>2</sub> tests	Equivalent range in water
Inlet pressure	MPa	6.60, 7.36, 8.36, 8.80	19.8, 22.1, 25.1, 26.4
Inlet temperature	°C	5 – 30	320 – 350
Outlet temperature	°C	20 – 60	350 – 435
Mass flux	kg m <sup>-2</sup> s <sup>-1</sup>	800, 1000, 1500	594, 1188, 1782
Heat flux	kW m <sup>-2</sup>	20 – 500	150 – 3800

### 5.2 Heat transfer and pressure drop measurements in the 8 and 22 mm tube test sections

Detailed measurements of wall temperature will be conducted in the 8 and 22 mm tubes over the nominal ranges of conditions that have been specified in Table 6. The full ranges of mass flux and heat flux may not be covered simultaneously for the 22 mm tube, because of limitations in the loop capabilities. The results will be compared to existing measurements in tubes and will complement and expand the available database. They will also serve as reference for comparisons with measurements in the rod bundle test section under the same conditions. In addition, these two test sections will be modified with the additions of two pressure taps each, one just before and a second one just after the heated sections, so that pressure drop can be measured under the test conditions. The pressure drop will be measured with a differential pressure transmitter (Omega Engineering, Inc., Model PX771A-300WCDI), having a range from 0 to 75 kPa and an uncertainty of 0.1%.

### 5.3 Heat transfer and pressure drop measurements in a rod bundle

The available rod bundle subassembly, shown in Figure 7, comprises a pressure tube with an inner diameter of 25.4 mm, which contains three directly heated rods and three wall inserts. The rod bundle has five sections, each 500 mm long, connected in series and separated from the neighbouring sections by endplates. Pads are positioned between the rods and on the rod sides that face the pressure tube at regular intervals to ensure that the gaps remain as uniform as possible. The first and last sections of the rod bundle are made of copper, whereas the three sections in the middle are made of Inconel, so that only these three sections are subject to significant direct heating. The rod diameter is 10.0 mm and the

pitch to diameter ratio is 1.14. The hydraulic diameter of the rod bundle is 6.7 mm and the flow area is 177 mm<sup>2</sup>. The ends of the three rods are fastened on copper plates, which are connected to the power supply. The inner surface of the pressure tube is electrically insulated. Each of the three rods in the last heated section of the rod bundle contains a sliding thermocouple assembly, as shown in Figure 8. This assembly consists of a carriage rod, near the upstream end of which two insulated K-type thermocouples are mounted across from each other. A loaded spring pushes each thermocouple against the heated surface to ensure good thermal contact. Each thermocouple may be rotated within the rod over 360° and traversed along the rod over a distance of 378 mm.

Heat transfer and pressure drop measurements in the rod bundle will be conducted over the same ranges of conditions as those listed in Table 6. The axial and azimuthal variations of wall temperature in the three rods of the last heated section will be measured and used to calculate the heat transfer coefficient. These results will be compared to available measurements in tubes and predictions of empirical correlations. Of particular interest will be to determine whether deteriorated heat transfer occurs in flow under supercritical pressures in rod bundles, and, if so, the conditions under which it does.

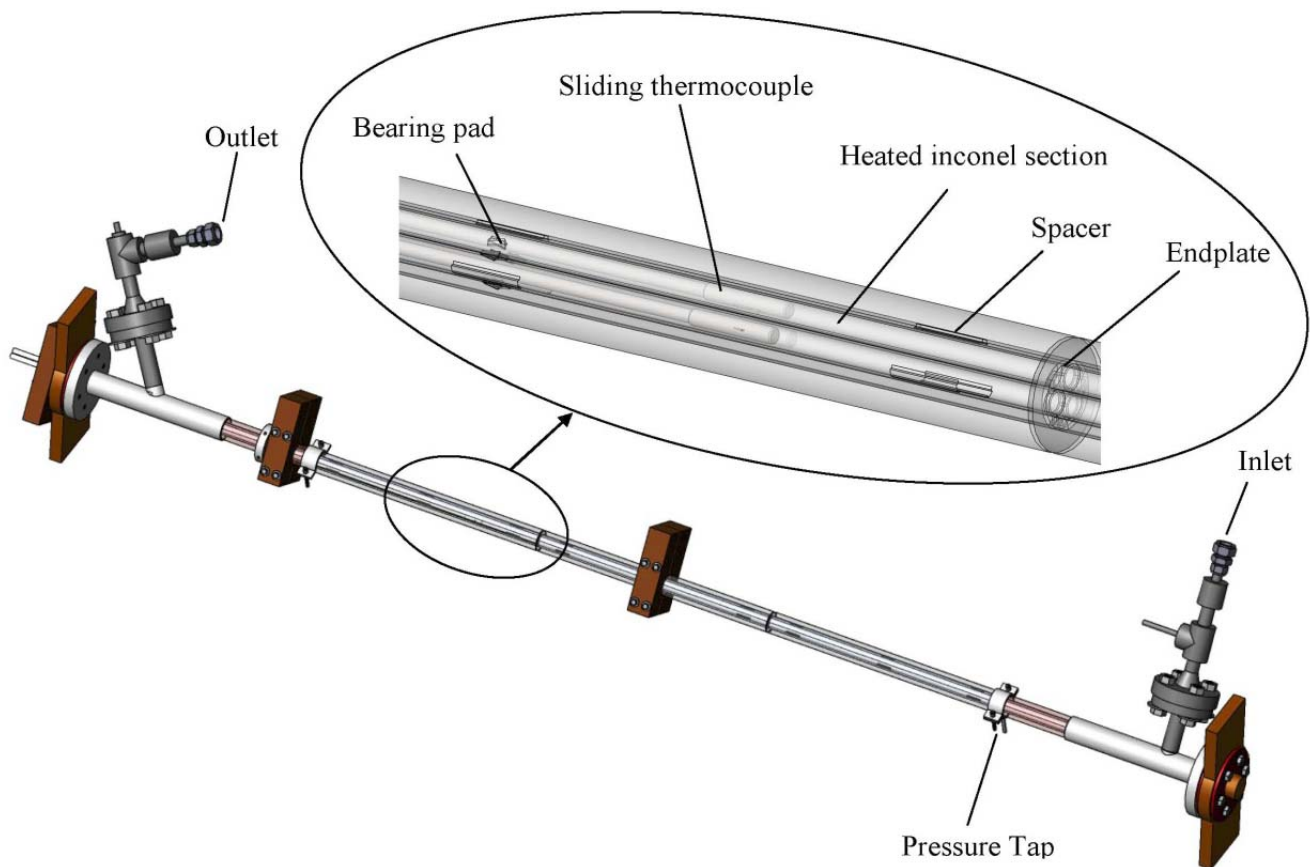


Figure 7 Rod bundle test section.

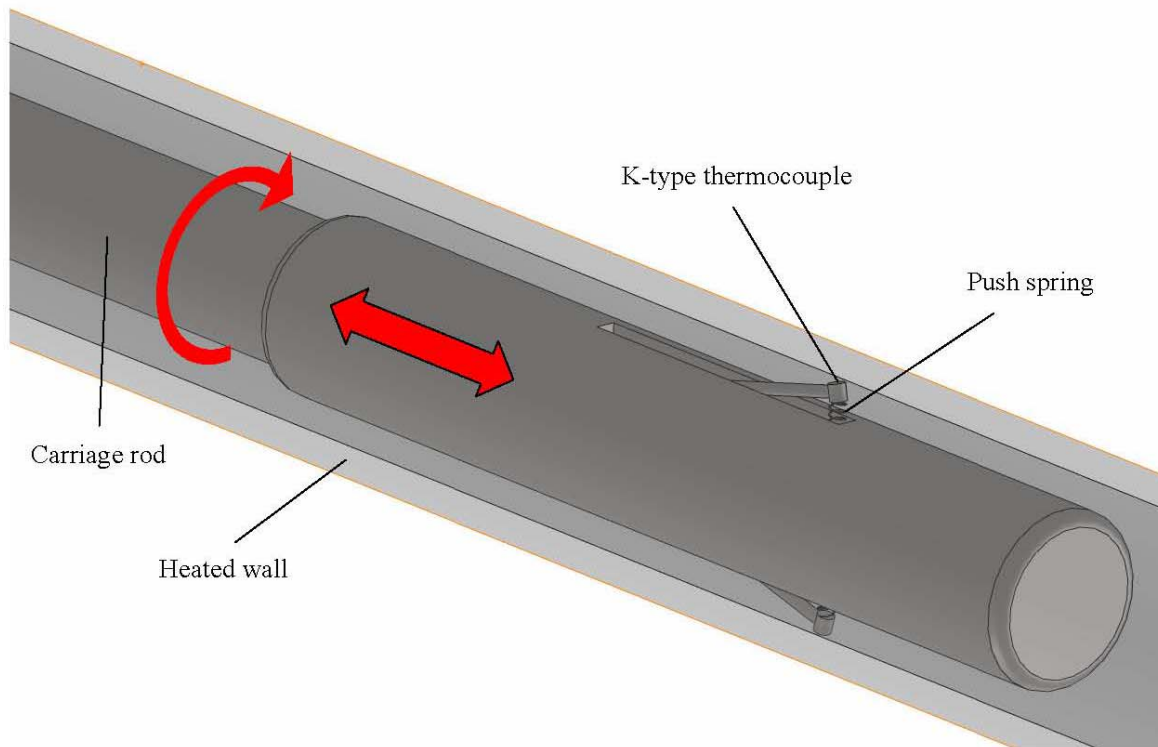


Figure 8 Sliding thermocouple assembly for rod-bundle.

#### 5.4 Measurements of turbulence and in-flow temperature in the 22 mm tube

Finally, the velocity and temperature fluctuations in the 22 mm ID test section will be measured with hot- and cold-wire probes, respectively. The velocity sensor will be operated in the constant temperature mode and the temperature sensor will be operated in the constant current mode. The design of these probes will be similar to the one used by Vukoslavčević et al. [4], who have also presented results of probe calibration and response under ranges of conditions comparable to those of interest in this work. Flanges mounted on the test section as shown in Figure 9 will be used for probe insertion. The probes will be electrically insulated from the test section as well as sealed to a pressure of at least 10 MPa. The calibration of the probes will be performed in situ against a micro-Pitot tube and a micro-thermocouple or micro-thermistor, which will be inserted and traversed in the test section together with the hot- and cold-wire probes. This set of measurements of velocity and temperature fluctuations are expected to contribute to the understanding of the complex phenomena of heat transfer enhancement and deterioration, which occur under certain conditions of interest to SCWR, and to serve as benchmarks for the validation of analytical models and numerical simulations.

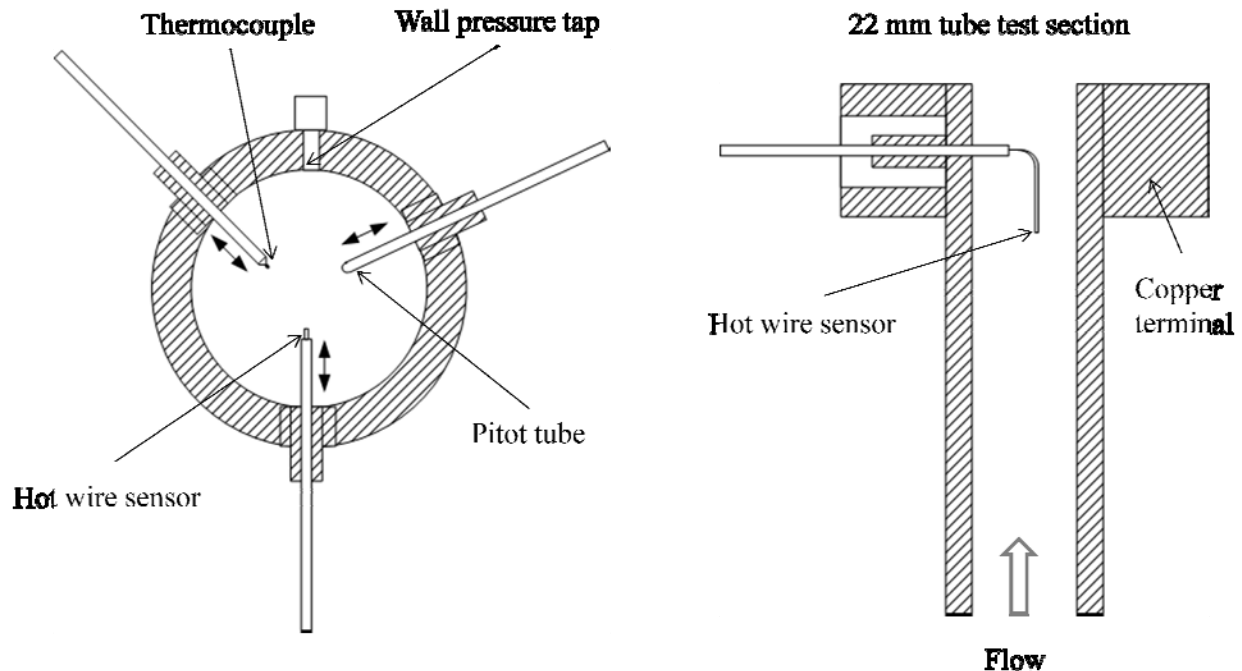


Figure 9 Schematic diagram of the probe insertion arrangement.

## 6. Summary

In this article we presented a detailed description of a new supercritical heat transfer facility using carbon dioxide as a medium. As part of the loop commissioning procedure, the heat transfer coefficient was measured for a relatively low mass flux in upward flow along a vertical 8 mm tube under both subcritical and supercritical conditions.

Under subcritical conditions, two heat transfer regimes were reproduced. For a relatively low heat flux, the fluid remained in the liquid phase and the heat transfer coefficient that was estimated from the experimental data was in fair agreement with predictions of the Dittus-Boelter correlation. For a higher heat flux, the fluid near the heated wall apparently boiled at some location in the test section, beyond which the experimental heat transfer coefficient was in fair agreement with predictions of the Dougall-Rohsenow correlation that applies to the film-boiling regime.

Under supercritical conditions with relatively low heat and mass fluxes, we observed an enhancement of heat transfer in the inlet region, where the wall temperature and the bulk temperature of CO<sub>2</sub> were both lower than the pseudo-critical temperature, and strong heat transfer deterioration further downstream. The streamwise variation of the experimental heat transfer coefficient had some qualitative resemblance with the predictions of the Jackson and Fewster correlation.

The article further describes our plans for measuring wall temperature variation and pressure drop in upward flows along tubes with inner diameters of 8 and 22 mm and a simple rod bundle under a variety of supercritical conditions, as well as plans for measuring turbulence and temperature fluctuations in the 22 mm tube.

## Acknowledgments

The financial support of NSERC, NRCan and AECL is gratefully acknowledged. We thank Noam Lightstone and Rachel Anderson for assisting us with the drawings and Hussam Zahlan for assistance with the analysis.

## References

- [1] I. L. Pioro and R. B. Duffey, "Heat Transfer and Hydraulic Resistance at Supercritical Pressures in Power-Engineering Applications", ASME Press, New York, 2007.
- [2] F. W. Dittus and L. M. K. Boelter, "Heat transfer in automobile radiators of the tubular type", University of California, Berkeley, Publications on Engineering, Vol. 2 (13), pp. 443-461, 1930.
- [3] I. Pioro, H. F. Khartabil and R. B. Duffey, "Heat transfer to supercritical fluids flowing channels – empirical correlations (survey)", Nuclear Engineering and Design, Vol. 230, pp. 69-91, 2004.
- [4] P. V. Vukoslavčević, I. M. Radulovic and J. M. Wallace, "Testing of a hot- and cold-wire probe to measure simultaneously the speed and temperature in supercritical CO<sub>2</sub> flow", Experiments in Fluids, Vol. 39 (4), pp. 703-711, 2005.

## Nomenclature

$C_p$	specific heat at constant pressure (J kg <sup>-1</sup> K <sup>-1</sup> )
$\bar{C}_p = \frac{i_w - i_b}{T_w - T_b}$	average specific heat (J kg <sup>-1</sup> K <sup>-1</sup> )
$G$	mass flux (kg m <sup>-2</sup> s <sup>-1</sup> )
$h$	heat transfer coefficient (kW m <sup>-2</sup> K <sup>-1</sup> )
$i$	specific enthalpy of CO <sub>2</sub> (kJ kg <sup>-1</sup> )
$D$	inner diameter of test section (mm)
$k$	thermal conductivity (W m <sup>-1</sup> K <sup>-1</sup> )
$L_h$	heated length (m)
$P$	pressure (MPa)
$q$	heat flux (W m <sup>-2</sup> )
$T$	temperature (°C)
$x_e$	equilibrium quality
$z$	axial coordinate (m)

### Greek letters

$\mu$	dynamic viscosity (kg m <sup>-1</sup> s <sup>-1</sup> )
$\rho$	density (kg m <sup>-3</sup> )

### Non-dimensional numbers

$Nu = \frac{hD}{k}$	Nusselt number
$Pr = \frac{\mu C_p}{k}$	Prandtl number
$\bar{Pr} = \frac{\mu \bar{C}_p}{k}$	average Prandtl number
$Re = \frac{GD}{\mu}$	Reynolds number

### Subscripts

<i>b</i>	bulk
<i>c</i>	critical
<i>f</i>	saturated liquid
<i>fb</i>	film boiling
<i>g</i>	gas
<i>hom</i>	homogeneous
<i>in</i>	inlet
<i>loss</i>	heat loss to or gain from the surroundings
<i>out</i>	outlet
<i>pc</i>	pseudo-critical
<i>sat</i>	saturation
<i>v</i>	vapour property evaluated at $(T_w + T_{sat})/2$
<i>w</i>	wall